Improving spatial resolution of strain-encoded (SENC) Magnetic Resonance Elastography (MRE) for enhancing stiff-mass detection

A. A. Harouni[1], J. Hossain[1], M. A. Jacobs[2], and N. F. Osman[1,2]

[1]Electrical and computer Engineering, Johns Hopkins University, Baltimore, MD, United States, [2]Department of Radiology, Johns Hopkins University, Baltimore, MD, United States

Introduction: According to the American Cancer Society's 2009 report, one in eight women will develop breast cancer in her lifetime. Early detection through periodic screening is the key to lower mortality-rates, which are expected to be 40,610 cases in 2009. Given the fact that cancer tumors are 3 to 13 times stiffer than both normal tissue and benign tumors [1], Fast Strain-Encoded (FSENC) MR with limited hardware was previously introduced by Fahmy et al [2] to detect difference in stiffness by directly measuring the strain. The hardware used a balloon and rubber bands to compress and uncompress the breast, which lead to inaccurate and unrepeatable compressions limiting both the scan resolution and the scan time to only one compression. In this work, we introduce new hardware capable of periodically compressing the breast allowing us to use Strain-Encoded (SENC) [3]. Our hardware allows us to prolong scan time leading to higher resolution, signal-to-noise ratio (SNR), and contrast-to-noise (CNR). Simple controls and multiple safety measures were added to ensure accurate, repeatable and safe in-vivo experiments.

Hardware: Our hardware uses two air-cylinders and a simple control circuit to produce accurate and repeatable compressions (see Fig. 1). For safety reasons, we use components that can handle 60 PSI, while operating them at 25 PSI. Our hardware consists of a scanner side and a patient side described below:

1) **Scanner side:** This part of the hardware is responsible for:
   a. Ensuring that the pressure does not exceed 30 PSI by monitoring the pressure using a pressure gauge. If pressure exceeds 30 PSI, the air is released outside the system through the three-way solenoid.
   b. Synchronizing with the scanner by generating ECG pulse, which allows us to tag the tissue at normal position, then acquire our image while tissue is at compressed position.
   c. Controlling the 4-way solenoid to direct the airflow in and out of the backward and forward chambers of the double acting cylinder, which produces periodic motion that compresses the breast.
2) **Patient side:** Our patient side casing fits under standard MR breast coils. We designed the patient casing so that it has maximum flexibility to accommodate different breast sizes (53mm up to 120mm in diameter) as well as different compression levels (15% up to 50% compression). Our system uses air-cylinders that have a stroke length of either 1" or 2". Moreover, different-sized adjustable plates (1/8", 1/4",1/2",3/4") can be added—either alone or with any combination—to shorten the air-cylinders' stroke length by constraining the cylinders motion. This allows us to control the maximum compression that is comfortable for each patient. Using air-cylinders provides us with a built in safety feature that guarantee the front plate will never crush the patient's breast. In addition, a normally closed patient switch (Fig.1) is added to allow the patient to disable the system by releasing the pressure in case of discomfort.

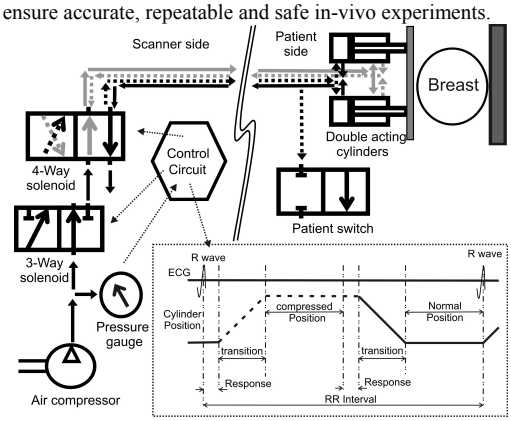

Fig.1: Block diagram for our hardware. Dotted lines show the airflow direction during the first half of the cycle where air fills backward chambers and deflating air from forward chamber making the front plate compress the breast; While solid lines shows the airflow direction during the second half of the cycle, where air flows into forward chamber and deflates from backward chamber retracting the front plate to normal position.

Experiments: We performed our scans at 3T MRI Philips scanner (Philips Medical Systems, Best, the Netherlands) using a four-channel phased-array breast coil. A custom-made phantom was designed to show SENC sensitive and accuracy. This phantom was made-out of gelatin with medium stiffness with six stiffer cuboids implanted in the middle. The cuboids were 8mm thick with varying sizes (2mm to 10mm). To determine the response time and the transient time of our system, we performed a steady state free precession (SSFP) scan with 10ms temporal resolution. By examining SSFP images, we set the tagging delay to 100 ms and the trigger delay=500 for the SENC and FSENC scan. Both SENC and FSENC had the same scanning parameters: FOV = 192×192, slice thickness=5mm with a Cartesian K-space acquisition, strain range of zero stretching to -36% compression, tagging frequency=0.354mm^{-1}, low and high tune images were acquired at frequencies 0.354mm^{-1} and 0.553mm^{-1}. In order to complete FSENC scan in only one compression, we used in-plain resolution of 2x2mm, TFE factor=25 and EPI factor=5. To maintain comparable SNR for SENC compared to FSENC—given the fact that SNR is proportional to the voxel size and the square root of the readout period—for SENC scan we used in-plain resolution=1x1mm, segmented K-space acquisition with TFE factor=10, EPI factor=3, and scan time=19 cycles. An extra SENC scan was performed without compressing the phantom. A standard T1 Weighted scan was also performed. We calculated SNR and tumor-CNR by $CNR = 2(S_{tumor} - S_{Background})^2 / (\sigma^2_{tumor} + \sigma^2_{Background})$. where, S and σ are the strain mean and standard deviation, respectively.

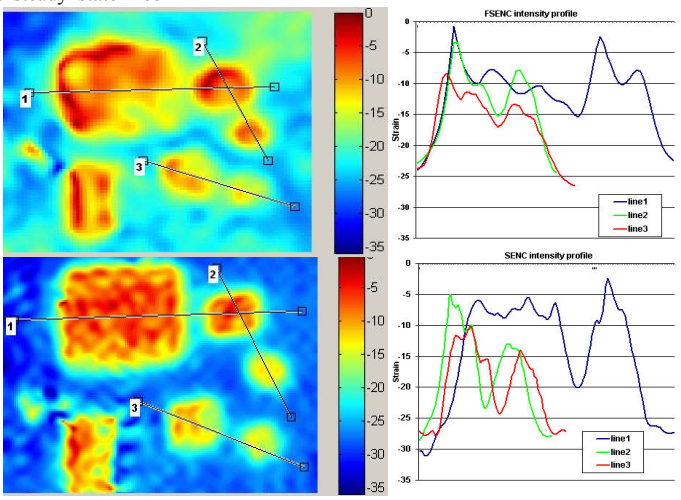

Fig.2: Strain images for low-resolution FSENC (top) and high-resolution SENC (bottom) with corresponding strain profile of 3 lines, each cuts through two tumors.

Results: Because our implants had the same T1 as the background, they were barely visible on the T1 image. Both FSENC and SENC images acquired with out compression did not show any signs of implants. This indicates that all the contrast in figures 2 is exclusively due to the strain difference between the tumors and the background. Mean SNR for SENC and FSENC were 70 and 45, respectively. Fig.2(left) shows the implants for both SENC and FSENC with three lines each going through two tumors with their strain profile (right). SENC strain profiles show two peaks that are clearly separated. While, FSENC strain profiles are distorted and can barely distinguish the two peaks. For all implants, SENC images had almost four times higher tumor-CNR than FSENC images (Fig.3).

Conclusion: We have introduced a novel hardware that enables us to achieve accurate and repeatable compressions of the breasts. It also allows us to increase the scanning time in order to achieve higher resolution, SNR, and CNR compared to images acquired using FSENC with the old hardware. Results show that high-resolution SENC images have four-fold CNR increase relative to low-resolution FSENC images, which leads to better tumor detection.

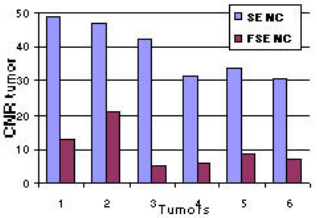

Fig.3: SENC and FSENC CNR for the 6 implants

References: [1] Samani A. et al, Phys. Med. Biol. 52:1565 (2007). [2] Fahmy A. et al, TBME 358(2004). [3] Osman N et al, Magn. Resn. Med. 46: 324-10 (2001).

Acknowledgment: The authors would like to thank Dr. AbdEl-Monem M. El-Sharkawy for his help with the hardware and thoughtful discussions. This work was supported in part by the following grants NHLBI R01HL072704, NIH 1P50HL08946, 1R01CA100184, and P50 CA103175.